Role of DAB2IP in modulating epithelial-to-mesenchymal transition and prostate cancer metastasis

Daxing Xie[a,b], Crystal Gore[a], Jun Liu[c], Rey-Chen Pong[a], Ralph Mason[c], Guiyang Hao[c], Michael Long[c], Wareef Kabbani[d], Luyang Yu[e], Haifeng Zhang[e], Hong Chen[f], Xiankai Sun[c], David A. Boothman[g], Wang Min[e,1], and Jer-Tsong Hsieh[a,h,1]

Departments of [a]Urology, [c]Radiology, [d]Pathology, and [g]Oncology, University of Texas Southwestern Medical Center, Dallas, TX 75390; [b]Department of General Surgery, Tongji Hospital, Tongji Medical College, Huazhong University of Science and Technology, Wuhan, Hubei 430030, China; [e]Interdepartmental Program in Vascular Biology and Transplantation and Department of Pathology, Yale University School of Medicine, New Haven, CT 06510; [f]Cardiovascular Biology Research Program, Oklahoma Medical Research Foundation, Oklahoma City, OK, 73104; and [h]Graduate Institute of Cancer Biology, China Medical University, Taichung 404, Taiwan, China

Edited by George R. Stark, Lerner Research Institute NE2, Cleveland, OH, and approved December 7, 2009 (received for review July 22, 2009)

A single nucleotide polymorphism in the *DAB2IP* gene is associated with risk of aggressive prostate cancer (PCa), and loss of DAB2IP expression is frequently detected in metastatic PCa. However, the functional role of DAB2IP in PCa remains unknown. Here, we show that the loss of DAB2IP expression initiates epithelial-to-mesenchymal transition (EMT), which is visualized by repression of E-cadherin and up-regulation of vimentin in both human normal prostate epithelial and prostate carcinoma cells as well as in clinical prostate-cancer specimens. Conversely, restoring DAB2IP in metastatic PCa cells reversed EMT. In DAB2IP knockout mice, prostate epithelial cells exhibited elevated mesenchymal markers, which is characteristic of EMT. Using a human prostate xenograft-mouse model, we observed that knocking down endogenous DAB2IP in human carcinoma cells led to the development of multiple lymph node and distant organ metastases. Moreover, we showed that DAB2IP functions as a scaffold protein in regulating EMT by modulating nuclear β-catenin/T-cell factor activity. These results show the mechanism of DAB2IP in EMT and suggest that assessment of DAB2IP may provide a prognostic biomarker and potential therapeutic target for PCa metastasis.

Prostate cancer (PCa) has surpassed lung cancer as the leading cancer among American men (1). In the absence of metastasis, prostate cancer is largely a treatable disease. Thus, early diagnosis of patients who will develop PCa metastasis could reduce the mortality and morbidity associated with this disease. The development of metastasis depends on the migration and invasion of cancer cells from the primary tumor into the surrounding tissue. To acquire such invasive abilities, carcinoma cells may acquire unique phenotypic changes such as epithelial-to-mesenchymal transition (EMT). EMT is a highly conserved cellular process that allows polarized, generally immotile epithelial cells to convert to motile mesenchymal-appearing cells. This process was initially recognized during several critical stages of embryonic development and has more recently been implicated in promoting carcinoma invasion and metastasis (2–4). During EMT, three major changes occur: (*i*) morphological changes from a cobblestone-like monolayer of epithelial cells to dispersed, spindle-shaped mesenchymal cells with migratory protrusions; (*ii*) changes of differentiation markers from cell–cell junction proteins and cytokeratin intermediate filaments to vimentin filaments and fibronectin; and (*iii*) acquisition of invasiveness through the extracellular matrix (4). Decreased E-cadherin expression or gain of vimentin expression is closely correlated with various indices of PCa progression, including grade, local invasiveness, dissemination into the blood, and tumor relapse after radiotherapy (5–8).

A recent study using genome-wide association data reveals that a single nucleotide polymorphism probe located in the first intron of DAB2IP gene associates with the risk of aggressive PCa (9). The functional role of DAB2IP in PCa is poorly understood. DAB2IP, also known as ASK1-interacting protein-1 (AIP1), a novel member of the Ras GTPase-activating protein family, has been implicated in cell-growth inhibition and apoptosis (10, 11). DAB2IP is down-regulated in various human cancers mainly because of altered epigenetic regulation of its promoter, such as by DNA hypermethylation and/or histone modification (12–17). Thus, it is very likely that DAB2IP functions as a tumor suppressor in cancer development; however, its role and mechanism in cancer metastasis is largely unknown. In the current study, we show that loss of DAB2IP facilitates EMT leading to PCa metastasis.

Results

DAB2IP Regulates EMT In Vitro. Cells undergoing an EMT or mesenchymal-to-epithelial transition (MET) experience transient morphologic and biologic changes that will modify cell polarity, contact with neighboring cells, and cell motility (18). These phenotypic changes are reminiscent of C4-2 transfectants stably expressing DAB2IP (D1 and D2), which displays a clear morphological transition from spindle-like fibroblastic (e.g., Neo) to cobblestone-like cells (e.g., D1 or D2) with well-organized cell contact and polarity (Fig. 1*A*). The effect of DAB2IP expression on increasing E-cadherin and reducing vimentin, fibronectin, and N-cadherin expression was noticed in PCa (i.e., C4-2) (Fig. 1*B* and Fig. S1*A*). Similar changes were observed in breast cancer (i.e., MDA-MB-231) and embryonic kidney (i.e., 293) cells as well (Fig. S1*C*). In contrast, when endogenous DAB2IP expression in three different immortalized human normal-prostate epithelial (i.e., PZ-HPV-7, RWPE-1, and PNT1-A) and PCa (i.e., PC-3) cells were knocked out, EMT was clearly detected based on changes in cell morphology and biomarker expression (Fig. 1 *D* and *E* and Fig. S2 *A–D*). Moreover, the expression of DAB2IP impacted on the in vitro cell motility significantly (Fig. 1*C* and Fig. S2*E*), which was not caused by its effect on cell growth (Figs. S1*B* and S2*E*). Taken together, these data indicate that DAB2IP is a potent EMT inhibitor.

DAB2IP Modulates Glycogen Synthase Kinase (GSK)-3β-β-Catenin Signaling Pathway. To dissect the possible mechanism of DAB2IP in EMT responses, we examined the effect of DAB2IP

Author contributions: D.X., X.S., W.M., and J.-T.H. designed research; D.X., C.G., J.L., R.-C. P., G.H., M.L., L.Y., H.Z., and H.C. performed research; R.M., D.A.B., and W.M. contributed new reagents/analytic tools; D.X., C.G., J.L., R.-C.P., R.M., G.H., M.L., W.K., L.Y., H.Z., H.C., X.S., D.A.B., W.M., and J.-T.H. analyzed data; and D.X. and J.-T.H. wrote the paper.

The authors declare no conflict of interest.

This article is a PNAS Direct Submission.

[1]To whom correspondence may be addressed. E-mail: jt.hsieh@UTSouthwestern.edu, or wang.min@yale.edu.

This article contains supporting information online at www.pnas.org/cgi/content/full/0908133107/DCSupplemental.

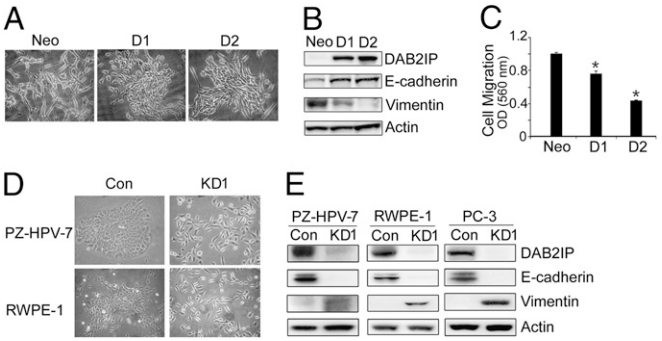

Fig. 1. DAB2IP regulates EMT in various cell lines. (*A*) Elevated DAB2IP reverses EMT in vitro. The morphology of C4-2 cells transfected with either control vector pCI-neo (Neo) or pCI-DAB2IP (D1, D2) was revealed by phase-contrast microscopy (magnification: 100×). (*B*) Expression of epithelial or mesenchymal markers in C4-2 (Neo, D1, and D2) sublines was analyzed by Western blotting. β-Actin was used as a loading control. (*C*) Effect of DAB2IP on cell migration in vitro. Neo, D1, and D2 cells were plated in Transwell chambers for 48 h, and quantitative measurements of migratory cells were determined. Data were presented as mean ± SEM of each sample measured in triplicate. (*D*) Knockdown of DAB2IP initiates EMT in vitro. PZ-HPV-7 and RWPE-1 cells were infected with control lentivirus or lentivirus-expressing shRNA specific to DAB2IP and then selected with puromycin. Morphology was revealed by phase-contrast microscopy (magnification: 100×). (*E*) Increased mesenchymal and reduced epithelial markers in DAB2IP-knockdown cells were analyzed by Western blotting.

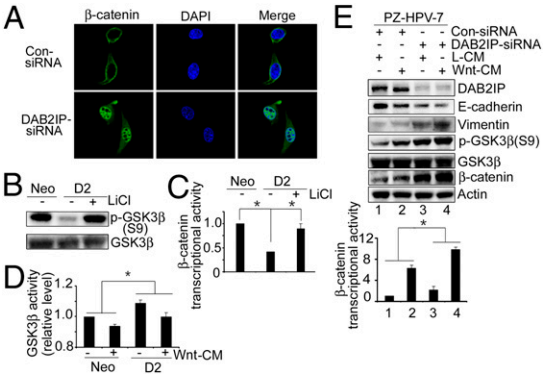

Fig. 2. DAB2IP activates GSK-3β and antagonizes Wnt-mediated EMT. (*A*) DAB2IP prevents β-catenin nuclear translocation. B16 mouse melanoma cells were transfected with control or DAB2IP-siRNA. Subcellular localization of β-catenin was visualized by confocal microscopy (magnification: 500×). (*B*) DAB2IP inhibits GSK-3β phosphorylation at S9. C4-2 sublines were treated with LiCl (20 mM) for 6 h, and cell lysates were blotted with p-GSK-3β (S9) and GSK-3β antibodies. β-Actin was used as a loading control. (*C*) DAB2IP inhibits β-catenin/TCF transcriptional activity. C4-2 sublines were transfected with TCF-responsive promoter reporter (TOP-flash) or non-responsive control reporter (FOP-flash) followed by LiCl treatment (20 mM; 6 h); then, luciferase activity was measured by the ratio of TOP and FOP. Relative luciferase activity is represented as mean ± SEM from each sample after normalizing with control (=1). Asterisk indicates statistical significance in Neo versus D2 cells ($P < 0.01$), as well as in D2 with versus without LiCl treatment ($P < 0.01$). (*D*) DAB2IP activates GSK-3β kinase activity. After treating C4-2 sublines with L- or Wnt-CM, GSK-3β was immunoprecipitated and kinase activities were determined as described in *Materials and Methods*. Relative GSK-3β kinase activities was represented as mean ± SEM from each sample after normalizing with untreated C4-2 (Neo; =1). Asterisks indicated statistical significance in Neo versus D2 cells ($P < 0.01$). (*E*) Knockdown of DAB2IP inactivates GSK-3β, promotes β-catenin activity, and enhances Wnt-induced EMT in PZ-HPV-7 cells. Cells were cotransfected with either control or DAB2IP-siRNA and TOP or FOP and then treated with L- or Wnt-CM. Cell lysates were subjected to Western blot. Relative luciferase analysis was performed as described above. Asterisks indicate statistical significance in cells transfected with control-siRNA cell versus DAB2IP-siRNA ($P < 0.05$).

on the GSK-3β-β-catenin signaling pathway. In canonical Wnt pathways, GSK-3β–mediated β-catenin degradation is inhibited, leading to accumulation of β-catenin in the nucleus that further transactivates β-catenin/T-cell factor (TCF) target genes. Thus, a hallmark of β-catenin signaling in both normal and neoplastic tissue is nuclear translocation (19). By knocking down endogenous DAB2IP levels with siRNA, we observed both accumulation of cytoplasmic β-catenin and nuclear translocation of β-catenin as well as reduced membrane-associated β-catenin (Fig. 2*A*). Although DAB2IP did not alter the steady-state levels of β-catenin mRNA (Fig. S3*A Left*) in D2 cells, cytoplasmic β-catenin levels substantially decreased, because DAB2IP can increase proteasomal degradation of β-catenin (Fig. S3*A Right*). Moreover, in DAB2IP-expressing cells, GSK-3β activity was significantly elevated based on Ser9 (S9, negative regulatory site) phosphorylation levels, β-catenin/TCF transcriptional activity (TOP/FOP), and GSK-3β kinase activity, respectively (Fig. 2 *B–D* and Fig. S3 *B* and *C*). Furthermore, DAB2IP diminished Wnt-elicited β-catenin/TCF transcriptional activity (Fig. S3*D*). Consistently, knocking down endogenous DAB2IP in PZ-HPV-7 cells by transient transfection of DAB2IP-siRNA increased GSK-3β phosphorylation (S9), β-catenin levels, and β-catenin/TCF transcriptional activity, which were further potentiated by Wnt treatment (Fig. 2*E*). Thus, DAB2IP modulates GSK-3β-β-catenin signaling through activation of GSK-3β by reducing S9 phosphorylation.

Wnt signaling is a key inducer of EMT during embryonic development and cancer progression (20–22). We tested whether or not manipulating DAB2IP levels in various cell lines could modulate Wnt-induced EMT. Whereas Wnt only slightly elicited EMT (Fig. 2*E*, lanes 1 and 2) in PZ-HPV-7 cells, its effect on EMT increased significantly after endogenous DAB2IP was knocked down by DAB2IP-siRNA (Fig. 2*E*, lanes 3 and 4). In contrast, restoring DAB2IP expression in 293 cells (DAB2IP-negative cell) prevented Wnt-induced EMT (Fig. S3*E*), strongly suggesting that DAB2IP was an antagonist of Wnt-mediated EMT.

DAB2IP Recruits PP2A to Active GSK-3β Through Its C2 Domain. Based on a screening using the Scansite program (http://scansite.mit.edu/) and coimmunoprecipitation (co-IP) (Fig. 3*A*), GSK-3β appears to directly associate with DAB2IP. Because DAB2IP is not a phosphatase, the mechanism of GSK-3β activation by DAB2IP is likely mediated by a separate phosphatase associated within this complex. We have previously shown that PP2A can form a complex with DAB2IP (23). PP2A is a heterotrimeric complex containing a catalytic subunit (*C*), a structural subunit (*A*), and a variable regulatory subunit (*B*) (24). Although some studies suggest GSK-3β (S9) as a potential substrate for PP2A (25–27), the functional role of PP2A in the Wnt-β-catenin pathway is still controversial (28). The co-IP data (Fig. 3*A* and Fig. S4 *A* and *D*) indicated that DAB2IP could form a complex with GSK-3β and PP2A as well as Axin. Structurally, DAB2IP contains several potential functional domains including an N-terminal pleckstrin-homology (PH) domain as well as C2, GTPase activating (GAP), C-terminal period-like (PER), proline-rich (PR), and leucine zipper (LZ) domains (Fig. 3*B*). By transfecting Flag-tagged DAB2IP deletion vectors (F, N, C, PHC2, and PH) into 293 cells, the data showed that C2 was the key domain that interacted with both GSK-3β and PP2A (Fig. S4*B*). Consistently, full-length DAB2IP, N, and PHC2 domains, rather than C and PH domains, inhibited β-catenin/TCF transcriptional activity (Fig. 3*C*). In addition, other mutant constructs, such as GAPm (GAP mutant) (10), S604A (S604 mutant) (29), and AAA (PR mutant) (29), did not inhibit β-catenin–mediated transcriptional activity (Fig. 3*C*), indicating

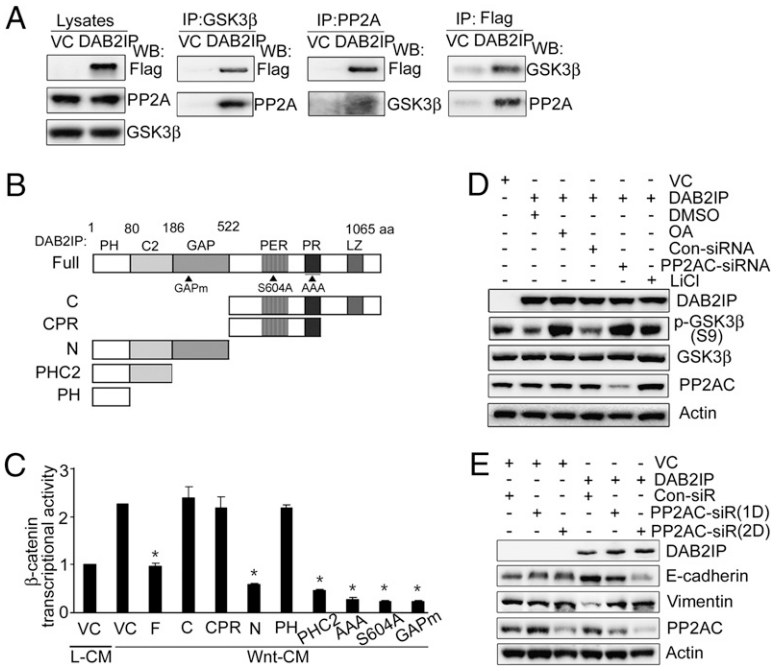

Fig. 3. PP2A is critical for DAB2IP-modulated GSK-3β-β-catenin signaling and EMT. (*A*) DAB2IP complexes are associated with both GSK3β and PP2A. Two hundred ninety-three cells were transfected with flag control vector (VC) or DAB2IP-F. Cell lysates were immunoprecipitated with GSK-3β, PP2A, and Flag antibodies and then probed with Flag and PP2A or GSK3β antibodies, respectively. (*B*) Schematic depiction of DAB2IP constructs containing different functional domains and mutants. (*C*) The effect of C2 domain of DAB2IP on β-catenin/TCF transcription activity. Two hundred ninety-three cells were cotransfected with various DAB2IP transfectants and TOP followed by L-CM or Wnt-CM treatment, and then, luciferase activity was determined. Asterisk indicates statistical significance in 293 cells transfected with VC versus F, N, and PHC2 domain ($P < 0.01$). (*D*) Endogenous PP2AC is critical for DAB2IP-mediated S9 phosphorylation of GSK-3β. Two hundred ninety-three cells transfected with either VC or DAB2IP were treated with OA (25 nM, 24 h) or LiCl (20 mM, 6 h) or cotransfected with PP2A-specific siRNA (100 pmol; 24 h). Cell lysates were subjected to Western blotting. (*E*) The role of PP2A in DAB2IP-modulated EMT. Two hundred ninety-three cells transfected with either VC or DAB2IP were cotransfected with PP2A-specific siRNA. Cell lysates were subjected to Western blotting.

that these functional domains were not involved in DAB2IP-modulated GSK-3β-β-catenin signaling.

To further assess the direct effect of PP2A on GSK-3β-β-catenin activity, 293 cells were cotransfected with several expression vectors: DAB2IP (*F*), GSK-3β [wild type (WT) or S9A, constitutive active], and PP2A [WT or catalytic inactive (LP)]. In the presence of both DAB2IP and GSK-3β-WT, PP2A-WT, rather than PP2A-LP, further decreased β-catenin/TCF transcriptional activity (Fig. S4*C*). GSK-3β-S9A was sufficient to inhibit β-catenin/TCF transcriptional activity; neither PP2A-WT nor PP2A-LP enhanced its inhibitory effect (Fig. S4*C*). We also examined the role of endogenous PP2A in DAB2IP-modulating GSK-3β-β-catenin signaling and MET responses. DAB2IP-expressing cells were treated with the PP2A inhibitor, Okadaic acid (OA), or PP2A-siRNA. Both OA and PP2A-siRNA treatments abolished DAB2IP-mediated dephosphorylation of GSK-3β on S9 (Fig. 3*D*). Consistently, either OA (Fig. S4*E*) or PP2A-siRNA (Fig. 3*E*) treatments alone could block DAB2IP-mediated MET responses. Similar results were also observed in PC-3 cells expressing endogenous DAB2IP (Fig. S4*F*). These data clearly indicate that PP2A is critical for DAB2IP-mediated GSK-3β activation and MET responses.

β-Catenin Overexpression Reverses DAB2IP-Mediated MET. Because DAB2IP can activate GSK-3β and then lead to decreased cytosolic β-catenin protein levels and nuclear β-catenin transcriptional activity (Fig. 2*A* and Fig. S5 *A-D*), we examined whether or not the inhibitory effect of DAB2IP could be reversed by overexpressing β-catenin. The elevated expression of β-catenin in PC-3 cells also induced EMT in a dose-dependent manner (Fig. S5*E*). Similarly, in both D2 and DAB2IP transfected cells, increasing dosage of β-catenin cDNA restored EMT based on marker and morphology (Fig. S6).

DAB2IP Down-Regulation Promotes Tumor Progression and Metastasis. Because PC-3 cells have low metastatic potential (30, 31) and the decreased DAB2IP expression in these cells can initiate EMT (Fig. 1*E*), we examined the metastatic potential of KD1- versus Con- expressing PC-3 cells using an orthotopic mouse model. Stable CMV–luciferase activity was confirmed in each subline to ensure the equal level before injection. Bioluminescent imaging (BLI) and small-animal positron emission tomography and computed tomography (PET-CT) were used to monitor tumor growth and onset of metastases. One week after injection, both BLI and 2-[^{18}F] fluoro-2-deoxy-D-glucose (^{18}F-FDG)-PET-CT (Fig. 4*A* and Fig. S7*A*) clearly detected multiple metastatic lesions in various organ sites in animals injected with PC-3-KD1 cells, and 3D imaging further revealed lymph-node metastases (Video S1). In contrast, control mice only exhibited small primary tumors 5 weeks postinjection, and none of them showed any signs of metastases (Fig. S7 *A* and *D*). Nearly all mice bearing DAB2IP-knockdown cells died within 2 weeks (Fig. S7*E*). From autopsy (Fig. 4*B* and Fig. S7 *B* and *C*), all mice bearing KD1 cells developed macroscopic evidence of enlarged mesenteric lymph nodes as well as additional lymph nodes in various organs, including the liver, kidney, and spleen; occasionally, some mice developed metastatic nodules in visceral organs including liver and stomach (Fig. S7*B*, green arrows). H&E data showed a definitive distant spread of PCa cells where poorly differentiated tumor cells were present within afferent lymph nodes (Fig. 4*C*). Immunohistochemistry (IHC) showed that the majority of tumor cells strongly expressed vimentin and p-GSK-3β (S9) (Fig. S7*F*), but they exhibited weak staining of E-cadherin and cytokeratin (Fig. 4*C*).

In addition, we also employed another PCa model (i.e., LAPC4) expressing androgen receptor (AR) and prostate-specific antigen (PSA) (32) to examine the effect of DAB2IP on cancer metastasis. By knocking down the endogenous DAB2IP, LAPC4 cells elicited similar EMT changes as those in PC-3 cells in vitro as well as a high incidence of lymph-node metastases using orthotopic KD1 tumor models (Fig. S8). These data provide a strong evidence for the inhibitory role of DAB2IP in PCa metastases.

DAB2IP Knockout Mice Exhibit Mesenchymal Characteristics in the Prostate Gland. To further determine the impact of DAB2IP on phenotypic changes in normal prostate glands, DAB2IP knockout (KO; DAB2IP$^{-/-}$) mice were employed (33). In DAB2IP WT (DAB2IP$^{+/+}$) mice, DAB2IP expression was associated with

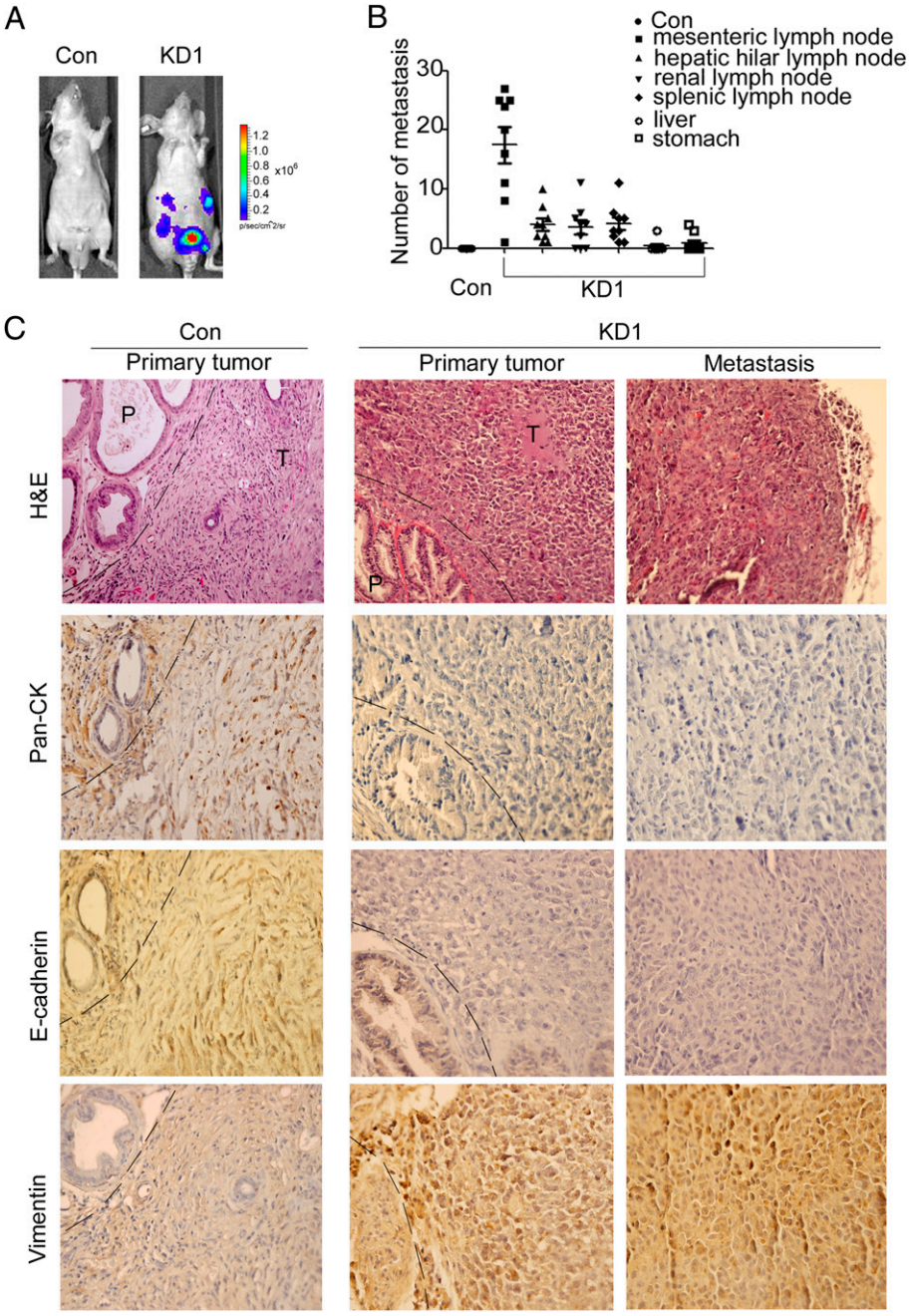

Fig. 4. DAB2IP down-regulation promotes tumor growth and metastasis. (*A*) Representative BLI imaging of mice bearing PC-3-KD1 tumors with multiple metastatic lesions. Mice (n = 9) were imaged 10 days later to determine local tumor growth and metastasis. (*B*) Numbers of metastatic nodules in individual mouse bearing Con or KD1 tumors at the time of sacrifice. (*C*) Representative H&E and IHC staining patterns. H&E staining showed primary tumor without detectable metastases in control mice and the lymph node metastases in mice bearing KD1 tumors 2 weeks postinjection (magnification: 100×). IHC showed the majority of KD1 tumors with a strong positive vimentin staining but weak E-cadherin and Cytokeratin staining (magnification: 200×). The dashed line separates between the area of mouse prostate (P) and PC-3 tumor (T).

prostate glandular epithelial cells (Fig. 5*A*). Consistent with in vitro data (Figs. 2 and 3), S9 phosphorylation of GSK-3β was higher in DAB2IP$^{-/-}$ than that in DAB2IP$^{+/+}$ mice (Fig. 5*B*), suggesting that GSK-3β activity was suppressed in DAB2IP$^{-/-}$ mice. Also, the prostate glandular epithelia in DAB2IP$^{-/-}$ mice exhibit decreased E-cadherin, elevated vimentin expression, and strong nuclear β-catenin staining (Fig. 5*A*). Although no spontaneous PCa has been detected in DAB2IP$^{-/-}$ mice, hyperplastic lesions were often detected in DAB2IP$^{-/-}$ mice older than 6 months of age (Fig. S9*A*).

We further examined the relationship between DAB2IP expression and EMT markers using different stages of human prostate specimens including normal tissue, benign prostatic hyperplasia (BPH), and PCa with moderate and poorly differentiated tumor. Loss of DAB2IP and E-cadherin as well as increased vimentin and p-GSK-3β were clearly detected in tissues from prostate-cancer patients (Fig. 5*C* and Fig. S9*B*). There is a significant correlation between the levels of DAB2IP and E-cadherin (r = 0.8390) and an inverse correlation between the levels of DAB2IP and vimentin (r = 0.7255) levels in all of the

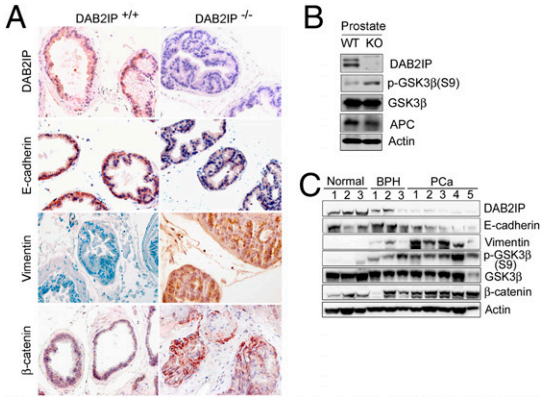

Fig. 5. DAB2IP KO mice exhibit mesenchymal characteristics in the prostate gland. (*A*) DAB2IP$^{-/-}$ mice express elevated mesenchymal markers in the prostate gland. Expression of DAB2IP, E-cadherin, Vimentin, and β-catenin in paraffin sections of prostate were determined by IHC (magnification: 400×). (*B*) Reduced GSK-3β activity in DAB2IP$^{-/-}$ mice. Prostate homogenate from WT and KO mice were subjected to Western blotting. (*C*) Loss of DAB2IP expression correlates with EMT marker changes in clinical specimens of prostate-cancer patients. Expression levels of DAB2IP, E-cadherin, vimentin, and β-catenin protein as well as p-GSK-3β(S9) levels in normal (n = 6), BPH (n = 6), and PCa (n = 10) tissues were determined by Western blotting. Densitometry was normalized with β-Actin level.

samples tested (Fig. S9*C*). Taken together, our human and mouse in vivo data are consistent with in vitro data from various normal epithelial or cancer-cell lines.

Discussion

In this study, we clearly show that DAB2IP functions as a scaffold protein in modulating GSK-3β-β-catenin signaling and EMT. In the presence of DAB2IP, interaction of its C2 domain with both PP2A and GSK-3β facilitates GSK-3β activation through S9 dephosphorylation. Then, it decreases nuclear β-catenin accumulation and its transcriptional activity, indicating the potent inhibitory function of DAB2IP in Wnt-β-catenin signaling. Within the DAB2IP-PP2A-GSK-3β complex, GSK-3β seems to be a direct substrate for PP2A, a known negative regulator in Wnt-β-catenin signaling (28, 34), which is the underlying mechanism for the DAB2IP function. The role of S9 phosphorylation of GSK-3β in Wnt/β-catenin signaling is still controversial. For example, the S9 phosphorylation of GSK-3β is not correlated with Wnt-mediated GSK-3β activity in certain cell types (35, 36). However, other studies have shown that many growth factors, such as insulin growth factor, transforming growth factor-β, and epidermal growth factor etc., can increase β-catenin accumulation through S9 phosphorylation of GSK-3β (37–40). Inactivation of GSK-3β through S9 phosphorylation is involved in hepatitis B virus-x protein (HBX)-mediated β-catenin stabilization in hepatocellular carcinoma cells (41). From several prostate-cell lines (e.g., C4-2 and PZ-HPV-7) tested, we showed that S9 phosphorylation of GSK-3β was clearly involved in DAB2IP-mediated β-catenin stability and transcriptional activity, suggesting that the effect of S9 phosphorylation on β-catenin signaling is cell-type dependent.

In general, β-catenin has a dual role in EMT: it not only enhances cell–cell adhesion by associating with cadherin complexes in adheren junctions of cell membrane, but it also functions as a transcriptional coactivator after interacting with TCF transcription factor complexes in the nucleus (21, 42). The induction of EMT by nuclear β-catenin has been explored during development in cell lines and tumors (2). Several studies suggest that β-catenin–mediated transcription can induce Slug (43) or Twist1 (44) gene expression that further represses E-cadherin, thereby contributing to the EMT. Our data show that loss of DAB2IP in cells can lead to the accumulation of nuclear β-catenin (Fig. 2*A* and Fig. S5*C*), because DAB2IP facilitates cytoplasmic β-catenin degradation (Fig. S3*A*). Thus, we believe that DAB2IP can modulate the dynamic switching between membrane- and nuclear-associated β-catenin through PP2A and GSK-3β (Fig. 2 and Fig. S5), which determines EMT (4). In addition, we observed that ZEB1 and ZEB2/SIP1, transcriptional factors associated with EMT (3, 4), were highly elevated in DAB2IP-depleted cells (Fig. S2*D*). Taken together, these data indicate that DAB2IP is a key regulator in preventing EMT.

The majority of human visceral tumors derived from carcinomas exhibit an epithelial phenotype. To break away from neighboring cells and invade adjacent tissue layers or peripheral lymph nodes, carcinoma cells often lose cell–cell adhesion and acquire motility. In general, 25–30% of patients newly diagnosed with PCa will have local invasive cancer, and almost all of these patients will eventually develop metastatic disease, accounting for most cancer deaths (1). Needless to say, the detection of metastatic lesions at an early stage or during treatment should lead to an increase in disease-free survival rates. From the clinical outcome of PCa progression, the presence of lymph-node invasion has the lowest rate of 10-year progression-free survival rate (45). Our orthotopic PCa animal model (Fig. 4) shows that mice bearing DAB2IP-knockdown cells have a dramatic increase in the incidence of lymph-node metastases as well as the number of metastatic sites where tissues clearly exhibit mesenchymal characteristics. Wnt signaling has been identified as a determinant of lung-cancer metastasis to brain and bone (46). Similarly, our data indicated that down-regulation of DAB2IP can increase the propensity of PCa cells to metastasize to lymph nodes (Fig. 4 and Fig. S8), which was associated with the hyperactivation of Wnt/β-catenin/TCF pathway (Fig. 2*E* and Fig. S5*D*). Consistently, DAB2IP$^{-/-}$ mice exhibit similar changes of EMT markers in the prostate gland (Fig. 5). In addition, prostate hyperplasia was observed in DAB2IP$^{-/-}$ mice after 6 months of age. A previous study has also shown the prostate hyperplasia in adenomatous polyposis coli knock-out (APC$^{-/-}$) mice after 4.5 weeks of age (47). In both models, the accumulation of nuclear β-catenin was observed; however, unlike PCa, which was detected in APC$^{-/-}$ mice after 7 months of age, no tumor has been detected in our model at this age. Because APC is known to regulate many pathways other than the Wnt/β-catenin pathway (48), it is possible that other downstream effects in addition to nuclear β-catenin activation may be involved in PCa formation in APC$^{-/-}$ mice. In DAB2IP$^{-/-}$ prostate, APC levels remained the same as in DAB2IP$^{+/+}$ mice (Fig. 5*B*) and thus, might also exert an inhibitory effect on tumor initiation.

In summary, this study delineates the functional role of DAB2IP in EMT, which also explains how loss of DAB2IP in PCa underlies the onset of aggressive metastatic PCa. We believe that the assessment of DAB2IP expression in PCa specimens can be a valuable prognostic biomarker for risk of PCa metastasis and the delineation of DAB2IP function could provide a potential intervention strategy for PCa metastasis.

Materials and Methods

Plasmid Constructs, Conditioned Medium, Antibodies, siRNA Oligonucleotides, and Immunoprecipitation. See *SI Materials and Methods*.

Cell Culture and Clinical Specimens. C4-2, DAB2IP-transfected C4-2 sublines (i.e., D1 and D2), the vector control subline (Neo), and PC-3 subline (Con, KD1) cells were maintained in *T* medium (Invitrogen) supplemented with 5% FBS. PZ-HPV-7 was maintained in PrEGM medium (Lonza). RWPE-1 cells were maintained in Keratinocyte medium (Invitrogen) containing 10% FBS. PNT1-A and human embryonic kidney 293 cells were maintained in Dulbecco's Modified Eagle's Medium (DMEM; Invitrogen) containing 10% FBS. MDA-MB-231 was maintained in RPMI medium (Invitrogen) containing 10% FBS.

The Institutional Review Board approved the tissue procurement protocol in this study, and appropriate informed consent was obtained from all patients. Benign prostatic hyperplasia specimens were obtained from transurethral prostatic resection, and primary cancer specimens (Gleason score of 6–9) were obtained from prostectomy performed in our institute. Cell lysates were subjected to Western blot analysis or immunohistochemical staining (*SI Materials and Methods*).

In Vitro Migration Assay. For migration assays, 5×10^4 cells were plated in the top chamber of a Transwell (24-well insert; pore size = 8 mm; Corning) and incubated with serum-free medium placed in the lower chamber. After incubation for 48 h, cells that did not migrate or invade through the pores were removed by a cotton swab, and cells on the lower surface of the membrane were stained with Cell Stain (Chemicon) and quantified by measuring OD_{560} with 96-well plate.

Analyses of Wnt Signaling Pathway. Cells were treated with Wnt-CM and L-CM for 24 h, and Wnt signaling activities were determined by various assays such as Western blot, qRT-PCR, GSK-3β kinase assay, Luciferase reporter gene assay, and fluorescence confocal microscopy (*SI Materials and Methods*).

Orthotopic Animal Model and Imaging. All experimental procedures have been approved by the Institutional Animal Care and Use Committee. The ventral prostate of male nu/nu mice (6–8 weeks of age) were exposed by midventral incision and injected with 5×10^5 cells suspended in 20 μL PBS. One week after injection, surgical staples were removed, and the tumor growth and local metastasis were monitored using BLI and PET (*SI Materials and Methods*).

Statistical Analysis. All error bars in graphical data represent mean ± SEM. Student's two-tailed *t* test was used for the determination of statistical relevance between groups, and $P < 0.05$ was considered significant.

ACKNOWLEDGMENTS. We thank Dr. Mien-Chie Hung for kindly providing GSK-3β plasmids, Dr. Jerry Shay for reading this manuscript, Erik A. Bey and Krista Hardy for editorial assistance, and Lin Yang and Shu-Fen Tseng for technical assistance. This work was supported by the U. S. Army Grant W81XWH-04-1-0222 (to J.-T.H.), the National Institutes of Health-supported Small Animal Imaging Research Program at University of Texas Southwestern (U24 CA126608), and in part by Department of Energy Grant DE-FG02-09ER64789 and National Institutes of Health Grant 5U19AI067773-04 (to D.A.B.).

1. Jemal A, et al. (2008) Cancer statistics, 2008. *CA Cancer J Clin* 58:71–96.
2. Thiery JP (2002) Epithelial-mesenchymal transitions in tumour progression. *Nat Rev Cancer* 2:442–454.
3. Thiery JP, Sleeman JP (2006) Complex networks orchestrate epithelial-mesenchymal transitions. *Nat Rev Mol Cell Biol* 7:131–142.
4. Yang J, Weinberg RA (2008) Epithelial-mesenchymal transition: At the crossroads of development and tumor metastasis. *Dev Cell* 14:818–829.
5. Tomita K, et al. (2000) Cadherin switching in human prostate cancer progression. *Cancer Res* 60:3650–3654.
6. Jaggi M, et al. (2006) N-cadherin switching occurs in high Gleason grade prostate cancer. *Prostate* 66:193–199.
7. Loric S, et al. (2001) Abnormal E-cadherin expression and prostate cell blood dissemination as markers of biological recurrence in cancer. *Eur J Cancer* 37:1475–1481.
8. Mason MD, Davies G, Jiang WG (2002) Cell adhesion molecules and adhesion abnormalities in prostate cancer. *Crit Rev Oncol Hematol* 41:11–28.
9. Duggan D, et al. (2007) Two genome-wide association studies of aggressive prostate cancer implicate putative prostate tumor suppressor gene DAB2IP. *J Natl Cancer Inst* 99:1836–1844.
10. Wang Z, et al. (2002) The mechanism of growth-inhibitory effect of DOC-2/DAB2 in prostate cancer. Characterization of a novel GTPase-activating protein associated with N-terminal domain of DOC-2/DAB2. *J Biol Chem* 277:12622–12631.
11. Xie D, et al. (2009) DAB2IP coordinates both PI3K-Akt and ASK1 pathways for cell survival and apoptosis. *Proc Natl Acad Sci USA* 106:19878–19883.
12. Chen H, Toyooka S, Gazdar AF, Hsieh JT (2003) Epigenetic regulation of a novel tumor suppressor gene (hDAB2IP) in prostate cancer cell lines. *J Biol Chem* 278:3121–3130.
13. Chen H, Tu SW, Hsieh JT (2005) Down-regulation of human DAB2IP gene expression mediated by polycomb Ezh2 complex and histone deacetylase in prostate cancer. *J Biol Chem* 280:22437–22444.
14. Dote H, et al. (2004) Aberrant promoter methylation in human DAB2 interactive protein (hDAB2IP) gene in breast cancer. *Clin Cancer Res* 10:2082–2089.
15. Dote H, et al. (2005) Aberrant promoter methylation in human DAB2 interactive protein (hDAB2IP) gene in gastrointestinal tumour. *Br J Cancer* 92:1117–1125.
16. Yano M, et al. (2005) Aberrant promoter methylation of human DAB2 interactive protein (hDAB2IP) gene in lung cancers. *Int J Cancer* 113:59–66.
17. Qiu GH, et al. (2007) Differential expression of hDAB2IPA and hDAB2IPB in normal tissues and promoter methylation of hDAB2IPA in hepatocellular carcinoma. *J Hepatol* 46:655–663.
18. Savagner P (2001) Leaving the neighborhood: Molecular mechanisms involved during epithelial-mesenchymal transition. *Bioessays* 23:912–923.
19. Logan CY, Nusse R (2004) The Wnt signaling pathway in development and disease. *Annu Rev Cell Dev Biol* 20:781–810.
20. Yardy GW, Brewster SF (2005) Wnt signaling and prostate cancer. *Prostate Cancer Prostatic Dis* 8:119–126.
21. Acloque H, Adams MS, Fishwick K, Bronner-Fraser M, Nieto MA (2009) Epithelial-mesenchymal transitions: The importance of changing cell state in development and disease. *J Clin Invest* 119:1438–1449.
22. Lee JM, Dedhar S, Kalluri R, Thompson EW (2006) The epithelial-mesenchymal transition: New insights in signaling, development, and disease. *J Cell Biol* 172:973–981.
23. Min W, et al. (2008) AIP1 recruits phosphatase PP2A to ASK1 in tumor necrosis factor-induced ASK1-JNK activation. *Circ Res* 102:840–848.
24. McCright B, Virshup DM (1995) Identification of a new family of protein phosphatase 2A regulatory subunits. *J Biol Chem* 270:26123–26128.
25. Welsh GI, Proud CG (1993) Glycogen synthase kinase-3 is rapidly inactivated in response to insulin and phosphorylates eukaryotic initiation factor eIF-2B. *Biochem J* 294:625–629.
26. Cross DA, et al. (1994) The inhibition of glycogen synthase kinase-3 by insulin or insulin-like growth factor 1 in the rat skeletal muscle cell line L6 is blocked by wortmannin, but not by rapamycin: Evidence that wortmannin blocks activation of the mitogen-activated protein kinase pathway in L6 cells between Ras and Raf. *Biochem J* 303:21–26.
27. Ikeda S, Kishida M, Matsuura Y, Usui H, Kikuchi A (2000) GSK-3beta-dependent phosphorylation of adenomatous polyposis coli gene product can be modulated by beta-catenin and protein phosphatase 2A complexed with Axin. *Oncogene* 19: 537–545.
28. Eichhorn PJ, Creyghton MP, Bernards R (2009) Protein phosphatase 2A regulatory subunits and cancer. *Biochim Biophys Acta* 1795:1–15.
29. Zhang H, et al. (2004) AIP1/DAB2IP, a novel member of the Ras-GAP family, transduces TRAF2-induced ASK1-JNK activation. *J Biol Chem* 279:44955–44965.
30. Kozlowski JM, et al. (1984) Metastatic behavior of human tumor cell lines grown in the nude mouse. *Cancer Res* 44:3522–3529.
31. Pettaway CA, et al. (1996) Selection of highly metastatic variants of different human prostatic carcinomas using orthotopic implantation in nude mice. *Clin Cancer Res* 2: 1627–1636.
32. Chen CD, et al. (2004) Molecular determinants of resistance to antiandrogen therapy. *Nat Med* 10:33–39.
33. Zhang H, et al. (2008) AIP1 functions as an endogenous inhibitor of VEGFR2-mediated signaling and inflammatory angiogenesis in mice. *J Clin Invest* 118:3904–3916.
34. Seeling JM, et al. (1999) Regulation of beta-catenin signaling by the B56 subunit of protein phosphatase 2A. *Science* 283:2089–2091.
35. Ding VW, Chen RH, McCormick F (2000) Differential regulation of glycogen synthase kinase 3beta by insulin and Wnt signaling. *J Biol Chem* 275:32475–32481.
36. McManus EJ, et al. (2005) Role that phosphorylation of GSK3 plays in insulin and Wnt signalling defined by knockin analysis. *EMBO J* 24:1571–1583.
37. Cheon SS, Nadesan P, Poon R, Alman BA (2004) Growth factors regulate beta-catenin-mediated TCF-dependent transcriptional activation in fibroblasts during the proliferative phase of wound healing. *Exp Cell Res* 293:267–274.
38. Desbois-Mouthon C, et al. (2001) Insulin and IGF-1 stimulate the beta-catenin pathway through two signalling cascades involving GSK-3beta inhibition and Ras activation. *Oncogene* 20:252–259.
39. Holnthoner W, et al. (2002) Fibroblast growth factor-2 induces Lef/Tcf-dependent transcription in human endothelial cells. *J Biol Chem* 277:45847–45853.
40. Papkoff J, Aikawa M (1998) WNT-1 and HGF regulate GSK3 beta activity and beta-catenin signaling in mammary epithelial cells. *Biochem Biophys Res Commun* 247: 851–858.
41. Ding Q, et al. (2005) Erk associates with and primes GSK-3beta for its inactivation resulting in upregulation of beta-catenin. *Mol Cell* 19:159–170.
42. van Es JH, Barker N, Clevers H (2003) You Wnt some, you lose some: Oncogenes in the Wnt signaling pathway. *Curr Opin Genet Dev* 13:28–33.
43. Conacci-Sorrell M, et al. (2003) Autoregulation of E-cadherin expression by cadherin-cadherin interactions: The roles of beta-catenin signaling, Slug, and MAPK. *J Cell Biol* 163:847–857.
44. Onder TT, et al. (2008) Loss of E-cadherin promotes metastasis via multiple downstream transcriptional pathways. *Cancer Res* 68:3645–3654.
45. Cheng L, et al. (2001) Risk of prostate carcinoma death in patients with lymph node metastasis. *Cancer* 91:66–73.
46. Nguyen DX, et al. (2009) WNT/TCF signaling through LEF1 and HOXB9 mediates lung adenocarcinoma metastasis. *Cell* 138:51–62.
47. Bruxvoort KJ, et al. (2007) Inactivation of Apc in the mouse prostate causes prostate carcinoma. *Cancer Res* 67:2490–2496.
48. Hanson CA, Miller JR (2005) Non-traditional roles for the Adenomatous Polyposis Coli (APC) tumor suppressor protein. *Gene* 361:1–12.